Directional coupling of optical signals by odd dark beams with mixed phase dislocations

D. Neshev[1], **A. Dreischuh**[1,*], **G.G. Paulus**[2,**], **H. Walther**[2,3,***]

[1] Sofia University, Dept. of Quantum Electronics, 5. J. Bourchier Blvd, 1164 Sofia, Bulgaria
[2] Max-Planck-Institut für Quantenoptik, Institut für Laserphysik, Hans-Korfermann-Str. 1, 85748 Garching, Germany
[3] Ludwig-Maximilians-Universität, Sektion Physik, Am Coulombwall 1, 85747 Garching, Germany

Abstract. Numerical simulations on the evolution of step-screw and edge-screw optical phase dislocations in bulk saturable self-defocusing nonlinear media are presented, with emphasis on their ability to induce steering waveguides for signal beams (pulses). Two schemes for directional coupling of such signals, both ensuring a reasonable coupling-to-cross-talk efficiency ratio, are investigated. The parameters useful for performance optimization of the couplers are discussed.

Dark spatial solitons (DSSs) formed in bulk self-defocusing Kerr-type nonlinear media (NLM) are able to guide co-propagating probe beams/pulses [1–3]. The underlying physical mechanism [4] is the intensity-dependent refractive-index change in a plane perpendicular to the propagation direction. Weak signal beams passing along these optically induced gradient waveguides [5] are subject to effective induced-phase modulation and are trapped. In photorefractive NLM [6], after the experimental generation of dark planar and vortex solitons in a quasi-steady-state regime [7], the situation is even more spectacular [8]. Because of the wavelength-dependent material response, DSSs generated at low powers but at a photosensitive wavelength are able to guide and steer much more powerful "signal" beams at non-photosensitive wavelengths. This is confirmed for photovoltaic [9], biased [10] and quasi-steady-state [11] photorefractive solitons and seems to hold also for incoherent dark solitons [12].

Both bright and dark beams can be forced to steer by introducing a spatial chirp to their transverse phase profiles with spatial light modulators [13–15]. When bright beams are guided by DSSs, the self-trapped dark beams create gradient waveguides that keep the bright beams narrow. This motivates the interest in investigating techniques for manipulating the transverse dynamics of dark beams. Arrays of one-dimensional DSSs generated by two intersecting plane waves in the regime of adiabatic amplification (and the probe beams guided by them) can be steered by changing the relative intensities of the interfering waves [16]. The transverse velocity of an optical vortex soliton (OVS) has a radial and an angular component arising from the transverse phase and intensity gradients, respectively [17, 18]. Two practical ways to control the vortex rotation have their origin in the Guoy phase shift on both sides of the background beam waist [18, 19] and in the interaction of ordered structures of OVSs [20] controlled by the topological charges. OVS steering is demonstrated by superposition of a weak background field [21]. Operation of planar Y-junction splitters for signal beams is demonstrated in both Kerr-type [22] and photorefractive NLM [23] with pairs of grey DSSs born from even initial conditions. The possibility to branch a single input probe beam into ordered structures of sub-beams by quasi-two-dimensional DSSs is demonstrated numerically in [24]. Other branching and steering schemes can be realized by employing the inherent dynamics of ring dark solitary waves [25], eventual NLM saturation [26] and/or anisotropy [27].

In this work we present numerical results on how one bright signal beam entering an input data channel can be guided and linked to a selected output port by a dark-beam-induced steering waveguide. A high steering speed of the induced waveguide can be obtained by using odd dark beams (ODBs) of finite lengths [28, 29] with a suitable choice of the mixed phase dislocation. Special attention is paid to ensure high energy efficiency of the directional coupler and short length of the interaction zone. Reconfiguration of the coupler is proposed to be done by changing the type of the phase dislocation reproduced by a multiple, active, single-voltage controlled computer-generated hologram [30].

1 Step-screw and edge-screw mixed phase dislocations

The mixed phase dislocations considered consist of a one-dimensional phase step of limited length, which ends, by

*Corresponding author.
(Fax: +35-92/962-5276, E-mail: ald@phys.uni-sofia.bg)
**(Fax: +49-89/3290-5200, E-mail: ggp@mpq.mpg.de)
***(Fax: +49-89/2891-4142, E-mail: prof.h.walther@mpq.mpg.de)

necessity, with pairs of phase semi-spirals with opposite helicities. In this work two possible cases are considered. The first phase dislocation of this type, which will be denoted step-screw (SS), is described by the phase distribution

$$\Phi_{\alpha,\beta}^{\mathrm{SS}}(x, y) = \Delta\Phi \left[\frac{1-\alpha}{2}\mathrm{sgn}(y) - \frac{\beta}{\pi}\arctan\left(\frac{\alpha y}{x+b\beta}\right) \right],$$
(1)

where the parameters α and β are defined as follows:

$$\alpha = \begin{cases} 0 & \text{for } |x| \leq b, \\ 1 \text{ and } \beta = -1 & \text{for } x > b, \\ 1 \text{ and } \beta = 1 & \text{for } x \leq -b. \end{cases}$$
(2)

The phase distribution

$$\Phi^{\mathrm{ES}}(x, y) = \frac{\Delta\Phi}{2\pi} \left[\arctan\left(\frac{y}{x+b}\right) - \arctan\left(\frac{y}{x-b}\right) \right],$$
(3)

will be referred to as edge-screw (ES). In (1)–(3) the quantity $\Delta\Phi$ stands for the magnitude of the step portion of the dislocation, $2b$ for its length, and x and y denote the transverse Cartesian coordinates parallel and perpendicular to the dislocation. Surface plots of the SS and ES phase dislocations are shown in Fig. 1a and b, respectively.

The formation of mixed phase dislocations was first identified by us in interferograms of decayed crossed one-dimensional DSSs in the presence of moderate saturation of the nonlinearity [31]. From our present point of view the classification [28] of such a formation generated via an instability as an ES or SS phase dislocation cannot be definitive. Both distributions shown in Fig. 1 are characterized by the same maximal phase difference $\Delta\Phi$ and dislocation length $2b$, but they differ in the rate $\partial\Phi/\partial\varphi|_{|x|>b}$ at which the phase changes azimuthally at their ends. In the step-screw case this change rate is twice as high as in the edge-screw case. In another
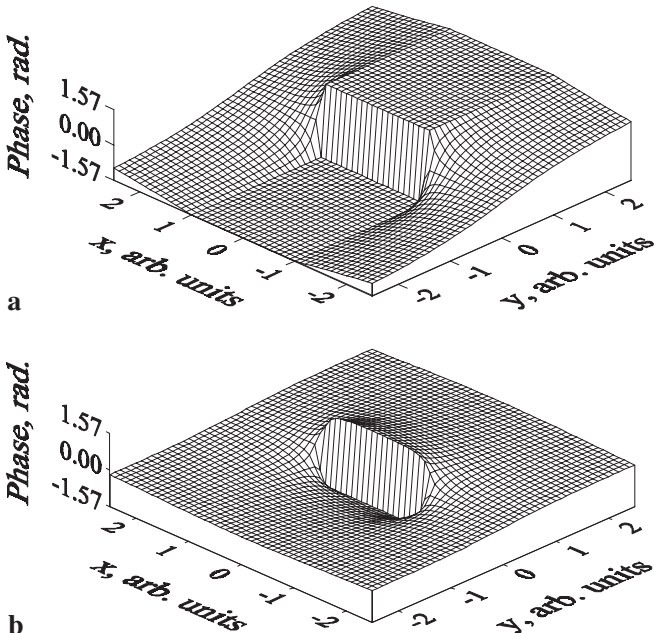
work [29] we found experimentally and confirmed numerically that in the interval $0.75\pi \leq \Delta\Phi \leq 1.25\pi$ the transverse steering velocity of an ODB of SS type is inversely proportional to $\Delta\Phi$. Because of the phase gradients across the edge portion of the dislocation the ES starts "immediately" steering. The step portion of the SS dislocation, however, is forced to steer by the outlying semi-helices. The process stabilizes after a propagation distance of the order of $1 L_{\mathrm{NL}}$ (see Figs. 2 and 3 in [28]), at a transverse velocity $2-3$ times smaller than in the ES case. In view of this, one more general statement holds: The transverse velocity of an ODB with mixed phase dislocation is inversely proportional to the absolute value of the azimuthal phase-change rate $\partial\Phi/\partial\varphi|_{|x|>b}$ outward from its ends. Therefore the identification of the type of ODBs generated as a result of an instability is not very reliable.

2 Initial conditions for the model

The $(2+1)$-dimensional evolution of the ODBs in bulk homogeneous, isotropic and saturable NLM is described by the nonlinear Schrödinger equation

$$i\frac{\partial E_{\mathrm{D}}}{\partial \zeta} + \frac{1}{2}\Delta_{\perp}E_{\mathrm{D}} - \frac{L_{\mathrm{Diff}}}{L_{\mathrm{NL}}}\frac{|E_{\mathrm{D}}|^2 E_{\mathrm{D}}}{(1+s|E_{\mathrm{D}}|^2)^{\gamma}} = 0,$$
(4)

where $\Delta_{\perp} = \partial^2/\partial\xi^2 + \partial^2/\partial\eta^2$. The transverse spatial coordinates are normalized to the initial dark beam width ($\xi = x/a$, $\eta = y/a$), and the nonlinear propagation path length ζ is expressed in units of Rayleigh diffraction lengths $L_{\mathrm{Diff}} = ka^2$. Furthermore, $L_{\mathrm{NL}} = (k|n_2|I_0)^{-1}$ is the nonlinear length, k is the wavenumber inside the NLM, and the background beam intensity at its entrance is normalized to that needed to form a 1D DSS of width a ($I_0 = I_{\mathrm{DSS}}^{\mathrm{1D}}$). In order to maintain correspondence to the conditions in our previous experimental works [29, 31], where NLM with saturation was used, we adopted the refractive-index correction

$$\Delta n = n_2|E_{\mathrm{D}}|^2/(1+s|E_{\mathrm{D}}|^2)^{\gamma},$$
(5)

with $s = 0.3$ and $\gamma = 3$. In a weak-signal approximation we took into account the bright-signal beam diffraction and the refractive-index changes it sees as induced by the ODB. In the NLM its evolution is described by

$$i\frac{\partial E_{\mathrm{B}}}{\partial \zeta} + \frac{1}{2}\frac{\lambda_{\mathrm{B}}}{\lambda_{\mathrm{D}}}\Delta_{\perp}E_{\mathrm{B}} - \sigma\frac{L_{\mathrm{Diff}}}{L_{\mathrm{NL}}}\frac{|E_{\mathrm{D}}|^2 E_{\mathrm{B}}}{(1+s|E_{\mathrm{D}}|^2)^{\gamma}} = 0.$$
(6)

The coupling coefficient σ depends on the nature of the physical process of the optical nonlinearity (e.g., molecular orientation, electronic response of bound electrons) and on the experimental conditions (e.g., the polarizations of the waves). The numerical simulations presented in this work refer to the wavelength ratio $\lambda_{\mathrm{B}}/\lambda_{\mathrm{D}} \simeq 1$ and $\sigma = 2$. The slowly-varying electric-field amplitudes of the ODBs were assumed to be tanh-shaped and of the form

$$E_{\mathrm{D}}(x, y, z=0) = \sqrt{I_0}B(r_{1,0}(x, y))\tanh\left(\frac{r_{\alpha,\beta}(x, y)}{a}\right)e^{i\Phi(x,y)},$$
(7)

where $\Phi(x, y) = \Phi_{\alpha,\beta}^{\mathrm{SS}}(x, y)$ for an SS phase dislocation, $\Phi(x, y) = \Phi^{\mathrm{ES}}(x, y)$ for an ES phase dislocation, and

Fig. 1. a Step-screw and **b** edge-screw mixed phase dislocations described by (1) and (3), respectively

$r_{\alpha,\beta}(x, y) = \sqrt{\alpha(x + \beta b)^2 + y^2}$ is the effective radial coordinate. In order to avoid any influence of the finite background beam of super-Gaussian form $B(r_{1,0}) = \exp\{-(\sqrt{x^2 + y^2}/w^2)^{14}\}$, its width was chosen to exceed the maximal ODB deflection at $\zeta = 10$ by more than 10 times. The signal beam is assumed to be sech-shaped and equal in width to the ODB width a. Its intensity is chosen to be one hundred times weaker than I_{DSS}^{1D}, thus not disturbing the dark beams by cross-phase modulation. In (4) and (6) negligible absorption is assumed, which holds if both L_{Diff} and L_{NL} are much shorter than the inverse of the absorption coefficient. The model equations are solved numerically by modification of the beam propagation method over a 1024×1024 grid.

Figure 2 shows the deflection of ODBs with ES and SS phase dislocations versus the nonlinear propagation path length $\zeta = z/L_{NL}$ for $b/a = 1.0$ (solid line), 2.0 (dashed line) and 3.0 (dotted line), normalized to the initial ODB width a. The difference between the transverse dynamics of the dark beams of different types is amazing. As already mentioned, it is due to the presence (in the ES case) or absence (in the SS case) of phase gradients across the one-dimensional portion of the dislocation at the entrance to the NLM. Besides, the transverse dynamics can be controlled by the type of the phase singularity in three possible ways [29]: by changing the b/a ratio, the phase step $\Delta\Phi$ and the background beam intensity. As can be seen in Fig. 2, changing the ODB length-to-width ratio offers an effective way to manipulate the ODB velocity. It is higher for the short and slower for the long dislocations. The long ones however could experience a transverse instability. More strongly pronounced is the increase in the velocity with decreasing magnitude of the step portion of the phase dislocation $\Delta\Phi$ [29], but we refrained from exploiting this. The reason is that during the steering process both types of ODBs inevitably become grey (and asymptotically disappear), which tends to destroy the coupler modeled. The numerical calculations performed showed similar but slightly weaker coupling efficiencies when the transverse deflection is controlled by $\Delta\Phi$ rather than by b/a. All the data in this work refer to $\Delta\Phi(\zeta = 0) = \pi$. Characteristic of the evolution of the ES phase dislocation is that it disturbs the background beam more weakly than the SS dislocation. In order to emphasize this, the number of gray-scale levels in the frames shown in Fig. 3 are intentionally reduced in the same way. The data refer to $\zeta = z/L_{NL} = 4$ and $b/a = 1$. The background beam

Fig. 3. Grey-scale plots of ES and SS ODBs with initial length-to-width ratio $b/a = 1$ after nonlinear propagation path length $\zeta = 4$. Some 3% of the total computational area are shown. See text for details

intensity in this simulation is chosen to correspond to that of a 1D DSS (I_{DSS}^{1D}). The dashed line is intended to underline that the ES ODB is more strongly deflected than the SS ODB.

The background beam intensity could be additionally used to control the dynamics of the ODBs, even their deflection does not strongly depend on it [29]. The background beam intensity, however, substantially influences the transverse beam profile and the guiding properties of the induced waveguide. Better spatial confinement could be expected at higher intensities. Numerical simulations were made to confirm this statement. Depending on the type of the dislocation (ES or SS) the highest encoupling efficiencies were achieved for levels $(1.25 \div 1.75)I_{DSS}^{1D}$. Higher intensities tend to destroy the induced waveguide due to the strong deformation of the dark beam profile under saturation of the nonlinearity.

The main task of the numerical simulations presented below is to find the proper parameter range for b/a and the beam intensity in order to reach maximal coupling efficiency in the analyzed schemes for directional coupling.

3 One-directional coupler

As a first step in this work we modeled the coupling of an input signal beam (pulse) to a desired output channel by optically induced waveguides. Figure 4a presents a simplified scheme for generating dark beam (DB) on a bright background beam (BB) by reproducing a reconfigurable computer-generated hologram (CGH), the subsequent combination with a signal beam/pulse (S) in front of the NLM, and the disposition of the imaginary output channels modeled. The change of the ODB steering direction in the NLM (i.e., the switching between channels with positive and negative numbers) is controlled by reversing the gradients of the screw portions of the dislocations. First, real implementation of this directional switching is feasible if there are reliable means to change the phase distributions of the ODBs. The electrically controllable, multiply-active, computer-generated holograms developed [30] are well suited for doing that. Because of the time needed to reconfigure the hologram, the relatively rare redirection of the data streams addressed to a desired channel will be preferable. Second, the energy efficiency of the guiding and switching should be as high as possible at the lowest possible cross-talk between the channels. The imaginary information channels considered to be coupled to the exit of the NLM are assumed to be rectangular with a width (height) 1.5 (3.0) times the input signal-beam FWHM.

The solid curves in Fig. 4b show transverse profiles of the naturally diffracting signal beam at $\zeta = 0$ and $10L_{Diff}$. For comparison, the dashed curve shows the intensity pro-
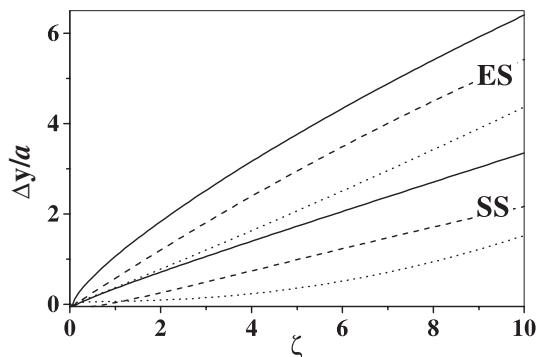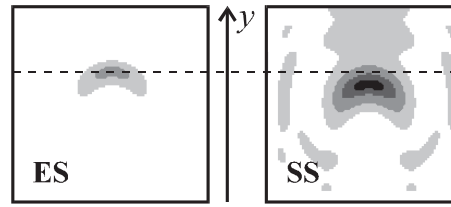

Fig. 2. Relative deflection of ODBs with edge-screw (ES) and step-screw (SS) phase dislocations versus nonlinear propagation path length $\zeta = z/L_{NL}$ for $b/a = 1.0$ (*solid line*), 2.0 (*dashed line*), and 3.0 (*dotted line*) at $\Delta\Phi = \pi$
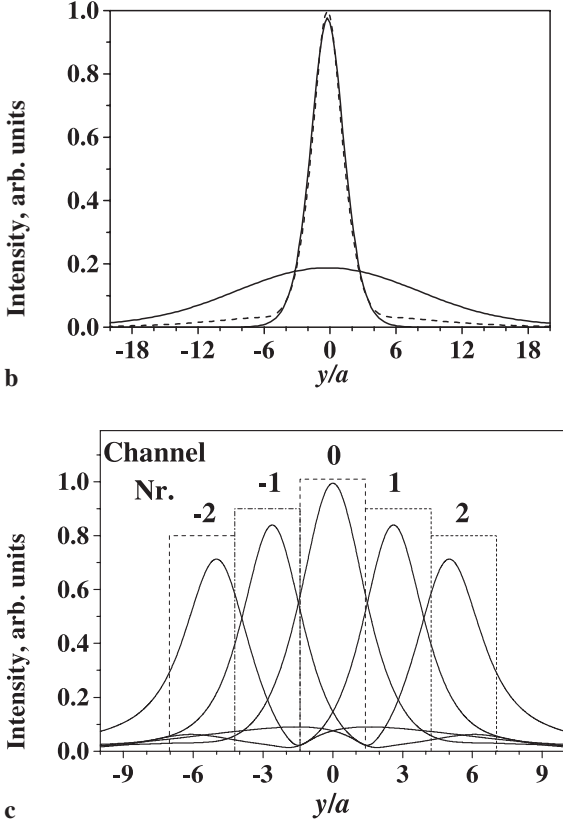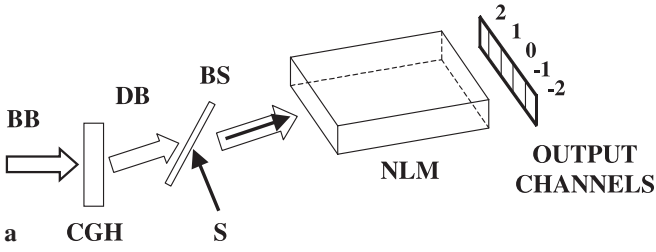
Fig. 4. a Simplified scheme for 1D directional coupling. BB: background beam; DB: dark beam; CGH: computer-generated hologram; BS: beam-splitter; S: signal beam; NLM: nonlinear medium. **b** Transverse intensity profiles of diffracting signal beam at $\zeta = 0$ and $10L_{\text{Diff}}$ (*solid curves*) and of a signal beam guided by an OV beam at $\zeta = 10$ (*dashed curve*). **c** Transverse profiles (along the steering direction y) of the signal beams coupled to one of the five output channels considered. The intensities are normalized to that of the signal in the direct channel 0; $\zeta = 10$

Table 1. One-directional coupler. Efficiencies (in %) in addressing channels 0, 1, and -2 by an OVS, SS ODB and ES ODB, respectively, and cross-talk efficiencies
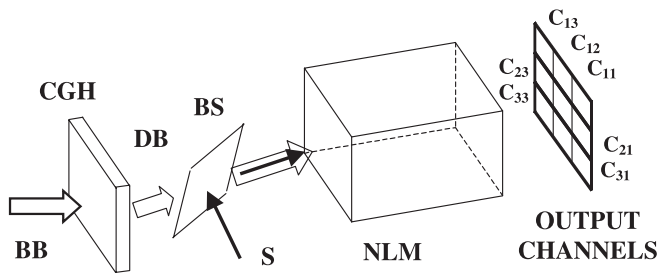
Channel guiding by	-2	-1	0	1	2	Energy losses
OVS	0.3	9.5	**74.7**	9.5	0.3	< 9.5
SS ODB	0.5	0.2	9.6	**70.7**	5.6	< 13.4
ES ODB	**52.2** (55.9)	14.1	1.4	1.6	0.8	< 29.9

input channel to channel 1, whereas this with an ES dislocation redirects the input to channel -2. The maximal efficiencies for channels 0, ± 1, and ± 2 to be expected are 74.7, 70.7 and 52.2%, respectively. In most channels the cross-talk signal should remain well below 14%. The ODB steering is accompanied by the creation of a leading dark wave and a trailing bright peak on the background beam (see Fig. 3 in [28]) which are more strongly pronounced in the SS case. The bright trailing peak pushes the signal beam stronger. This qualitatively explains the relatively high efficiency of the coupling to channels $+1$ and -1. Because of the additional self-defocusing of this peak it appears more effective to address channels $+2$ and -2 by ES ODBs. If the outlying channels are 2.25 times larger than the input signal beam width a, in the ES case the efficiency in coupling the signal to them can be increased by 3.6% to 55.9%. Due to the numerical discretization the overall accuracy in estimating the energies is within 0.02% and the coupling efficiencies in the respective channels are correct to within ± 0.04%.
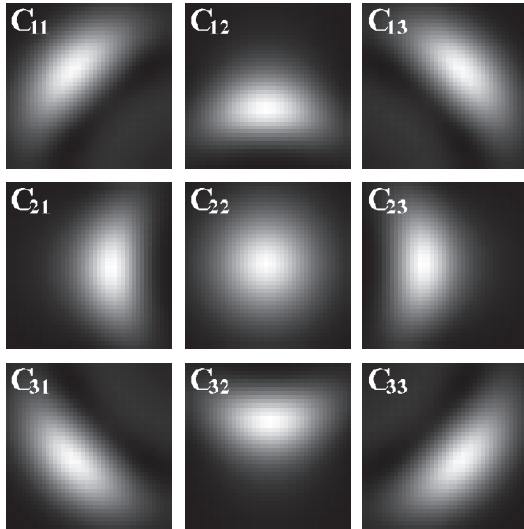
We should note here that because of the saturation of the nonlinearity the width of the induced waveguide is larger than in the case of pure Kerr nonlinearity. If a Kerr medium is considered (i.e. $s = 0$) the coupling efficiencies increase by 10%, whereas the cross-talk coefficients become slightly weaker.

4 Two-directional coupler

The interaction configuration modeled to address a desired channel from an imaginary array of information channels (3×3 in this work) is presented in Fig. 5a. In Fig. 5b we show the composition of grey-scale images of the signal beam coupled to each output port. The data below refer to $\zeta = 10$ and square channels of width and height 1.5 times the input signal beam FWHM. Best spatial confinement of the signal beams is achieved at a background beam intensity 1.5 times higher than that needed to form a 1D DSS of width a. Besides being controlled by the type of the phase dislocation (screw, ES, SS), the ODB transverse velocity and deflection at the exit of the NLM are adjusted by the initial ODB length-to-width ratio $2b/a$ ($b/a = 1.5$ in the SS case; and $b/a = 3.4$ in the ES case; both at $\Delta\Phi = \pi$). Let us denote the channels as C_{IJ}, where I and J are the respective row and column indices (see Fig. 5a). The central output channel C_{22}, which is on axis with respect to the input one, is addressed by an OVS [2, 3], and the side channels C_{21}, C_{23}, C_{12} and C_{32} by ODBs with appropriately $\pm 90°$ rotated SS phase dislocations; in contrast, signal beam coupling to each of the diagonal channels C_{11}, C_{13}, C_{31} and C_{33} is performed by ODBs with ES phase dislocations rotated $\pm 45°$. The calculated coupling efficiencies

file of a signal beam guided by an OVS up to $\zeta = 10$ for $I = 1.5I_{\text{DSS}}^{1D}$. Figure 4c shows the positions and the forms of the weak signal beams guided by the corresponding dark ones after a nonlinear propagation path length $\zeta = 10$. Channel 0 is assumed to be supported by an OVS [2, 3] with background intensity $1.5I_{\text{DSS}}^{1D}$, and channels 1 and -1 by ODBs with SS phase dislocations of $b/a = 1.5$ at $I = 1.5I_{\text{DSS}}^{1D}$; in contrast, channels 2 and -2 are considered to be induced by ODBs with ES phase dislocations with $b/a = 2.5$ at $I = 1.25I_{\text{DSS}}^{1D}$. The respective positions of the output ports along the steering direction (the arrow in Fig. 3) are sketched as rectangles.

The results for the directional coupling and cross-talk efficiencies obtained as ratios of the transmitted energy in a particular channel to the total one are summarized in Table 1. The ODB with a SS phase profile is assumed to couple the

Fig. 5. a Simplified scheme for 2D directional coupling. The notations are the same as in Fig. 4a. **b** Composition of grey-scale images of the signal beams at the exit of the two-directional coupler. Each channel is addressed separately, and the coupler length is $\zeta = 10$

are summarized in Table 2. The maximal values to be expected for the direct channel C_{22}, the neighboring channel C_{23}, and the diagonal channel C_{11} are 61.6, 49.6 and 47.1%, respectively, at cross-talk signals remaining well below 12%. Coupling the input channel to information channel C_{11} (by an ES ODB) should result in undesired but equal cross-signals in channels C_{IJ} and C_{JI} ($I \neq J$). If the input signal is coupled to channel C_{23}, the same should hold for channels C_{1J} and C_{3J}. The data obtained indicate that the discretization in our simulations leads to a maximal inaccuracy in the estimation of the coupling efficiencies that is within $\pm 0.04\%$. If pure Kerr nonlinearity is considered the coupling efficiencies are 1 to 8% higher. One reason for their decrease with increasing steering angle is the assumed initial flat phase fronts of the input signal beams. The efficiency can be increased by tilting the signal

phase fronts properly in order to improve the ability of the signal beams to follow the induced waveguide that moves in the transverse direction. Experimentally, an additional spatial light modulator placed prior to the beam-splitter (not shown in Figs. 4a and 5a) should be reconfigured in accordance with the type of the phase dislocation reproduced by the CGH.

5 Conclusion

The numerical data on the nonlinear evolution of mixed step-screw and edge-screw phase dislocations under equivalent conditions show an amazing difference between the transverse steering dynamics of SS and ES ODBs. Such odd dark beams are able to induce steering conduits for weak information beams (pulses) in bulk nonlinear media. As a result, two different schemes for directional coupling are proposed. The relatively high coupling and moderate cross-talk efficiencies in both of them provide a reasonable basis for further optimization and may open the way to constructing parallel reconfigurable all-optical logical elements.

Table 2. Two-directional coupler. Efficiencies (in %) in addressing channels C_{22}, C_{23} and C_{11} by an OVS, SS ODB and ES ODB, respectively, and cross-talk efficiencies

Channel guiding by	C_{11}	C_{12}	C_{13}	C_{21}	C_{22}	C_{23}	C_{31}	C_{32}	C_{33}	Energy losses
OVS	1.3	7.3	1.3	7.3	**61.6**	7.3	1.3	7.3	1.3	< 4.0
SS ODB	0.2	2.4	12.6	0.1	6.1	**49.6**	0.2	2.4	12.6	< 13.7
ES ODB	**47.1**	5.5	0.7	5.5	0.3	0.5	0.7	0.5	0.5	< 38.6

References

1. G.A. Swartzlander, Jr., C.T. Law: Phys. Rev. Lett. **69**, 2503 (1992)
2. A.H. Carlsson, J.N. Malmberg, D. Anderson, M. Lisak, E.A. Ostrovskaya, T.J. Alexander, Yu. Kivshar: Opt. Lett. **25**, 660 (2000)
3. C.T. Law, X. Zhang, G.A. Swartzlander: Opt. Lett. **25**, 55 (2000)
4. Y.S. Kivshar, B. Luther-Davies: Phys. Rep. **298**, 81 (1998)
5. A.W. Snyder, L. Poladian, D.J. Mitchell: Opt. Lett. **17**, 789 (1992); A.W. Snyder, A.P. Sheppard: Opt. Lett. **18**, 482 (1993); A.W. Snyder, S.J. Hewlett, D.J. Mitchell: Phys. Rev. Lett. **72**, 1012 (1994)
6. A.A. Zozulya, D.Z. Anderson: Phys. Rev. A **51**, 1520 (1995)
7. G. Duree, M. Morin, G. Salamo, M. Segev, B. Crossignani, P. Di Porto, E. Sharp, A. Yariv: Phys. Rev. Lett. **74**, 1978 (1995)
8. M. Shih, Z. Chen, M. Mitchell, M. Segev, H. Lee, R.S. Feigelson, J.P. Wilde: J. Opt. Soc. Am. B **14**, 3091 (1997)
9. M. Taya, M.C. Bashaw, M.M. Fejer, M. Segev, G.C. Valley: Phys. Rev. A **52**, 3095 (1995)
10. Z. Chen, M. Shih, M. Segev, D.W. Wilson, R.E. Muller, P.D. Maker: Opt. Lett. **22**, 1751 (1997)
11. M. Morin, G. Duree, G. Salamo, M. Segev: Opt. Lett. **20**, 2066 (1995)
12. Z. Chen, M. Mitchell, M. Segev, T.H. Coskun, D.N. Christodoulides: Science **280**, 889 (1998)
13. P. Mamyshev, A. Villeneuve, G. Stegeman, J. Aitchison: Electron. Lett. **30**, 726 (1994)
14. L. Friedrich, G.I. Stegeman, P. Millar, C.J. Hamilton, J.S. Aitchison: Opt. Lett. **23**, 1438 (1998)
15. Y. Li, Y. Chen, R.R. Alfano: Opt. Lett. **16**, 438 (1991)
16. C. Bosshard, P. Mamyshev, G. Stegeman: Opt. Lett. **19**, 90 (1994); see also P. Mamyshev, C. Bosshard, G. Stegeman: J. Opt. Soc. Am. B **11**, 1254 (1994)
17. Y.S. Kivshar, J. Christou, V. Tikhonenko, B. Luther-Davies, L.M. Pismen: Opt. Commun. **152**, 198 (1998)
18. D. Rozas, C.T. Law, G.A. Swartzlander, Jr.: J. Opt. Soc. Am. B **14**, 3054 (1997)
19. B. Luther-Davies, R. Powles, V. Tikhonenko: Opt. Lett. **19**, 1816 (1994)
20. D. Neshev, A. Dreischuh, M. Assa, S. Dinev: Opt. Commun. **151**, 413 (1998)

21. V. Tikhonenko, N. Akhmediev: Opt. Commun. **126**, 108 (1996); J. Christou, V. Tikhonenko, Y.S. Kivshar, B. Luther-Davies: Opt. Lett. **21**, 1649 (1996); see also I.V. Basistiy, V.Y. Bazhenov, M.S. Soskin, M.V. Vasnetsov: Opt. Commun. **103**, 422 (1993)
22. B. Luther-Davies, Y. Xiaoping: Opt. Lett. **17**, 496 (1992)
23. M. Taya, M.C. Bashaw, M.M. Fejer, M. Segev, G.C. Valley: Opt. Lett. **21**, 943 (1996)
24. D. Neshev, A. Dreischuh, S. Dinev, L. Windholz: J. Opt. Soc. Am. B **14**, 2869 (1997)
25. A. Dreischuh, V. Kamenov, S. Dinev: Appl. Phys. B **63**, 145 (1996); V. Kamenov, A. Dreischuh, S. Dinev: Phys. Scr. **55**, 68 (1997)
26. Y.S. Kivshar, V.V. Afanasjev: Opt. Lett. **21**, 1135 (1996); see also W. Krolikowski, X. Yang, B. Luther-Davies, J. Breslin: Opt. Commun. **105**, 219 (1994)
27. A.V. Mamaev, M. Saffman, A.A. Zozulya: Phys. Rev. Lett. **78**, 2108 (1997)
28. A. Dreischuh, G.G. Paulus, F. Zacher, I. Velchev: Appl. Phys. B **69**, 113 (1999)
29. A. Dreischuh, D. Neshev, G.G. Paulus, H. Walther: J. Opt. Soc. Am. B **17**, 2011 (2000)
30. C. Slinger, P. Brett, V. Hui, G. Monnington, D. Pain, I. Sage: Opt. Lett. **22**, 1113 (1997)
31. A. Dreischuh, G.G. Paulus, F. Zacher: Appl. Phys. B **69**, 107 (1999)